INSOMNIA

Sleep-Wake Differences in Relative Regional Cerebral Metabolic Rate for Glucose among Patients with Insomnia Compared with Good Sleepers

Daniel B. Kay, PhD[1]; Helmet T. Karim, BS[2]; Adriane M. Soehner, PhD[1]; Brant P. Hasler, PhD[1]; Kristine A. Wilckens, PhD[1]; Jeffrey A. James, BS[3]; Howard J. Aizenstein, MD, PhD[1]; Julie C. Price, PhD[3]; Bedda L. Rosario, PhD[5]; David J. Kupfer, MD[1]; Anne Germain, PhD[1]; Martica H. Hall, PhD[1]; Peter L. Franzen, PhD[1]; Eric A. Nofzinger, MD[1,4]; Daniel J. Buysse, MD[1]

[1]Department of Psychiatry, Sleep and Chronobiology Center, University of Pittsburgh School of Medicine, Pittsburgh, PA; [2]Department of Bioengineering, University of Pittsburgh, Pittsburgh, PA; [3]Department of Radiology, University of Pittsburgh, Pittsburgh, PA; [4]Cerêve Inc. Oakmont, PA; [5]Department of Epidemiology, Graduate School of Public Health, University of Pittsburgh, Pittsburgh, PA

Study Objectives: The neurobiological mechanisms of insomnia may involve altered patterns of activation across sleep-wake states in brain regions associated with cognition, self-referential processes, affect, and sleep-wake promotion. The objective of this study was to compare relative regional cerebral metabolic rate for glucose ($rCMR_{glc}$) in these brain regions across wake and nonrapid eye movement (NREM) sleep states in patients with primary insomnia (PI) and good sleeper controls (GS).

Methods: Participants included 44 PI and 40 GS matched for age (mean = 37 y old, range 21–60), sex, and race. We conducted [^{18}F]fluoro-2-deoxy-D-glucose positron emission tomography scans in PI and GS during both morning wakefulness and NREM sleep at night. Repeated measures analysis of variance was used to test for group (PI vs. GS) by state (wake vs. NREM sleep) interactions in relative $rCMR_{glc}$.

Results: Significant group-by-state interactions in relative $rCMR_{glc}$ were found in the precuneus/posterior cingulate cortex, left middle frontal gyrus, left inferior/superior parietal lobules, left lingual/fusiform/occipital gyri, and right lingual gyrus. All clusters were significant at $P_{corrected} < 0.05$.

Conclusions: Insomnia was characterized by regional alterations in relative glucose metabolism across NREM sleep and wakefulness. Significant group-by-state interactions in relative $rCMR_{glc}$ suggest that insomnia is associated with impaired disengagement of brain regions involved in cognition (left frontoparietal), self-referential processes (precuneus/posterior cingulate), and affect (left middle frontal, fusiform/lingual gyri) during NREM sleep, or alternatively, to impaired engagement of these regions during wakefulness.

Keywords: FDG, PET, insomnia, neuroimaging

Citation: Kay DB, Karim HT, Soehner AM, Hasler BP, Wilckens KA, James JA, Aizenstein HJ, Price JC, Rosario BL, Kupfer DJ, Germain A, Hall MH, Franzen PL, Nofzinger EA, Buysse DJ. Sleep-wake differences in relative regional cerebral metabolic rate for glucose among patients with insomnia compared with good sleepers. *SLEEP* 2016;39 (10):1779–1794.

Significance

This study builds on prior polysomnography and neuroimaging studies by using the high spatial resolution of positron emission tomography to address critical questions on the pathophysiology of insomnia. This study provides a detailed description of sleep-wake differences in relative regional glucose metabolism in good sleepers and patients with primary insomnia. Compared with good sleeper controls, we found that insomnia is associated with altered sleep-wake differences in relative glucose metabolism in major nodes of the default mode and executive control networks. These regionalized and state-specific findings add to the growing body of literature that suggests insomnia is a true sleep disorder with a complex and potentially multifaceted pathophysiology. These findings may inform new models of and novel treatments for insomnia.

INTRODUCTION

Insomnia disorder is defined as a persistent complaint of difficulty initiating or maintaining sleep, associated with daytime impairment or distress, and not accounted for by inadequate opportunity or circumstances for sleep.[1,2] Chronic insomnia disorder affects approximately 10% of adults[3] and is associated with cognitive impairments, reduced work productivity, lower quality of life, comorbid mental disorders, higher health care costs, and increased mortality risk.[4,5] The mechanisms through which insomnia is associated with these negative outcomes remains unclear, in part due to limited knowledge of the pathophysiology of insomnia itself.

Some clues to the pathophysiology of insomnia may be derived from its clinical features. Impairments associated with insomnia can be categorized into cognitive (e.g., episodic memory retrieval, working memory, planning, and naming),[6,7] self-referential (e.g., rumination),[8] affective (depression and altered positive/negative valence),[9,10] and sleep-wake promotion (sleep initiation/maintenance difficulties) domains. The first three domains are associated with brain regions that most consistently involve left frontoparietal, anterior and posterior cingulate, and temporal cortices.[11–18] Structures more critically involved in sleep-wake promotion, at the whole brain level, include brainstem, hypothalamic, and thalamic nuclei.

Neuroimaging studies of normal sleep provide a basis for investigating the pathophysiology of insomnia and its clinical features. Compared with wakefulness, nonrapid eye movement (NREM) sleep is associated with reduced cerebral blood flow and glucose metabolism in several brain regions related to cognition (frontoparietal regions), self-referential processes (frontoparietal, anterior cingulate, insular, temporal, and precuneus/posterior cingulate regions), affect (orbitofrontal cortex, medial temporal, and insular regions), and sleep-wake promotion (thalamus, hypothalamus, basal forebrain, basal ganglia, brainstem, and cerebellum).[19–29] Changes in blood flow/metabolism during NREM sleep are mainly thought to reflect decreased activity of cognitive, affective, and arousal systems[19,30] but may also reflect region-specific, use-dependent sleep intensity. Under normal circumstances, sleep-promoting and wake-promoting systems are thought to be mutually inhibitory. However, coactivation of these systems can be induced by threat or stress, as demonstrated by an animal model of acute insomnia.[31]

Thus, insomnia could plausibly involve heightened activation of arousal systems, reduced use-dependent sleep intensity, or coactivation of sleep- and wake-promoting processes during NREM sleep. In each of these scenarios, insomnia may involve smaller wake-NREM sleep differences in relative glucose metabolism in brain regions that typically show decreases during NREM sleep relative to wake.[32,33]

Other imaging modalities, such as structural and functional magnetic resonance imaging during wake or NREM sleep, have also been used to address the pathophysiology of insomnia and its daytime symptoms. Although these studies have used different criteria for insomnia, used different imaging methods, and reported some inconsistent findings, several studies have implicated alterations in structures or circuits related to cognition, self-referential processes, affect, and sleep-wake promotion.[34–49] However, a consistent set of brain regions or pattern of regional brain activity across wake and NREM sleep has not yet been identified in association with insomnia.

Only one prior neuroimaging study has investigated regional brain activity during both wake and NREM sleep in insomnia. Using the [^{18}F]fluoro-2-deoxy-D-glucose (FDG) positron emission tomography (PET) method, Nofzinger and colleagues reported that, relative to good sleeper controls (GS; n = 12), patients with primary insomnia (PI; n = 7) had smaller NREM sleep-wake differences in relative glucose metabolism in the medial frontal cortex, medial temporal lobe, insula, hypothalamus, thalamus, and brainstem.[33] Results from that study, although preliminary, are consistent with the hypothesis that insomnia involves an altered pattern of activity in brain regions most strongly associated with affective processing and sleep-wake promotion.[32]

In this study, we sought to test whether insomnia involves altered patterns of regional glucose metabolism across sleep-wake states in a larger sample of participants. Based on the clinical features of insomnia, current models of sleep-wake neurobiology, and previous neuroimaging studies on insomnia, we hypothesized that, compared with GS, PI would have altered patterns of relative glucose metabolism between wake and NREM sleep in brain regions involved in cognition, self-referential processes, affect, and sleep-wake promotion.

METHODS

Participants

Participants in this study included individuals with PI, determined by a structured clinical interview in accordance with Diagnostic and Statistical Manual of Mental Disorders, 4th edition (DSM-IV) criteria (PI; n = 44),[50] and GS who had no symptoms of insomnia, determined by a Pittsburgh Sleep Quality Index (PSQI) score < 5 (GS, n = 40). Demographic and clinical characteristics are presented in Table 1. In brief, participants were young to middle-aged adults (mean = 37 y, range 21–60), 58% female, and 82% white. Groups were well matched for age, sex, and race.

Participants were drawn from eight protocols conducted at the University of Pittsburgh between 1998 and 2012 that used the FDG-PET method[51] for studying regional brain metabolism in sleep-wake states (MH24652 helped fund all studies, MH61566 funded two studies, PSE00001 funded one study, and HL65112 funded one study). Protocols were approved by the Institutional Review Board and the Human Use Subcommittee of the Radiation Safety Committee at the University of Pittsburgh. Participants gave written informed consent and were compensated for participation.

Exclusion criteria for the current analyses were: (1) age younger than 18 y or older than 60 y, (2) self-reported left-handedness, (3) self-reported sleep disorders (other than insomnia for the PI group), (4) apnea-hypopnea index ≥ 15, (5) periodic limb movements with awakening ≥ 20/h, (6) caffeine > 400 mg per day on average, (7) inability to abstain from tobacco and alcohol during the study, (8) inability to abstain from drugs known to affect sleep for at least 2 w before participation (4 w for fluoxetine), (9) positive pregnancy test for women, and (10) presence of a significant current medical or psychiatric condition.

We identified a potential analysis sample of 104 participants who had either a morning wake or NREM sleep PET scan and met the aforementioned inclusion/exclusion criteria. From this sample, 20 participants were excluded based on criteria specific to the current analyses: having only a wake (n = 7) or NREM sleep (n = 2) PET scan, occurrence of REM sleep during the NREM sleep FDG uptake period (n = 3), or technical problems involving the wake (n = 2) or NREM sleep (n = 6) PET scan, such as limited field of view (FOV), low FDG dose, or co-registration complications. There were no significant group differences in the percentage or pattern of unusable scans.

Procedures

Participant demographics, clinical characteristic, and sleep quality were assessed with validated self-report questionnaires. To rule out sleep, psychiatric, and medical disorders, all participants were also assessed with validated clinician-administered questionnaires and interviews, overnight polysomnography (PSG), and medical history/physical examination.

Clinical Interview

The Structured Clinical Interview for DSM-IV Axis I Disorders was used to assess current and past history of psychiatric disorders.[52] Participants were free of current psychiatric disorders. Participants were not excluded from this study for a prior psychiatric history. Among PI, prior history included depression (n = 7), anxiety (n = 1), and substance use (n = 2) disorders. One GS had a prior psychiatric history including depression, anxiety, and substance use disorders.

Mood Measures

Instruments used to measure the severity of anxiety (Beck Anxiety Inventory,[53] a standard Visual Analog Scale for Anxiety, or the State-Trait Anxiety Index - Form Y-1[54]) and depression (Beck Depression Inventory,[55] Inventory of Depressive Symptomatology,[56,57] or Profile of Mood States-depression score[58]) symptoms differed across protocols. The total scores for each measure (minus sleep items) were converted to standard ordinal scales delineating minimal from mild-moderate levels of anxiety or depression severity.[59–63] Although having a current psychiatric diagnosis was exclusionary, 51% of the PI

group had mild-moderate symptoms of anxiety or depression compared to only 10% of the GS group (Table 1).

Sleep Measures

The PSQI was used to assess sleep quality over the past month.[64,65] The PSQI is a well-validated, 18-item self-report measure. Scores range from 0 to 21, with higher scores denoting worse sleep quality. A score greater than 5 indicates clinically significant levels of sleep disturbance.[66]

The Pittsburgh Sleep Diary was used to measure daily sleep onset latency, wake-time after sleep onset, total sleep time, time in bed, and sleep efficiency.[67] Participants were instructed to complete the diaries each morning directly after rising from bed. Sleep diary variables reported in Table 1 represent values averages across 7 nights.

Participants completed at least three overnight sleep studies, including screening/adaptation, baseline, and FDG-PET nights using standard procedures described in detail previously.[68] Sleep apnea and periodic limb movement disorder were screened during the initial screening/adaptation PSG night. Sleep apnea was assessed with a nasal pressure transducer, oronasal thermistor, fingertip oximeter, and respiratory inductance plethysmograph. Periodic limb movements were assessed with bilateral anterior tibialis electrodes. Sleep features other than apnea-hypopnea index and periodic limb movement arousal index were not compared across groups on the screening night due to well-characterized effects of adaptation on sleep.[69] Standard PSG-assessed sleep features (described in the next paragraphs) were assessed on a subsequent uninterrupted baseline night. An overnight FDG-PET night occurred on average 2 nights following the baseline night (range, 1 to 16 nights). Nightly urine screens were conducted to confirm that participants were free of alcohol and recreational drugs and that female participants were not pregnant.

Although the study protocols from which these data were extracted used slightly different PSG montages (e.g., some studies recorded the full PSG montage on all nights whereas others included a simplified PSG montage following the screening/adaptation night), core components were consistent across studies. The PSG montage included the C4/A1-A2 electroencephalogram (EEG) channel, bilateral electro-oculograms referenced to A1-A2, and submental electromyogram. These PSG signals were digitized and visually scored for staging in 20-sec epochs according to validated procedures by sleep technicians who were blinded to participant group.[70] All studies were scored according to Rechtschaffen and Kales criteria because the American Academy of Sleep Medicine scoring rules had not yet been published at the time the earliest studies were conducted.

The criterion for PSG-assessed sleep onset latency was the number of minutes from lights out until sleep onset, defined as the start of the first stage 2 NREM sleep epoch followed by at least 10 min of sleep (NREM stages 2–4 or REM sleep) interrupted by no more than 2 min of wake or stage 1. Sleep onset latency was calculated for both the baseline night and the NREM sleep PET scan night. Wake-time after sleep onset was the number of minutes scored as wake between sleep onset and the final sleep wake-up time according to PSG criteria. Total sleep time was the number of minutes spent in any PSG sleep stage following sleep onset until the final awakening. Time in bed was the number of minutes between lights out and final wake-up time. Sleep efficiency was defined as [(total sleep time / time in bed) × 100]. On the NREM sleep PET night, PSG was only collected directly before and during the uptake period. Thus, only sleep onset latency was assessed for that night, which was used to help determine whether the NREM sleep PET night differed from the baseline night in regard to this sleep feature.

Neuroimaging Protocol

The FDG-PET method used in this study has been described in detail in previous publications.[51,71,72] Structural MRI data were collected using either a 1.5 Tesla (T) GE Signa (GE Medical Systems, Milwaukee, WI) or 3.0 T Siemens Magnetom TIM Trio (Siemens Medical Systems, Malvern, PA) scanner. Participants were positioned in a standard head coil and received either a volumetric spoiled gradient recalled echo (three-dimensional [3D]-SPGR) pulse sequence in the 1.5 T scanner (n = 48) or a magnetization-prepared rapid acquisition with gradient echo (MPRAGE) pulse sequence in the 3 T scanner (n = 36). The 3D-SPGR sequence was optimized for maximal contrast of gray matter, white matter, and cerebrospinal fluid and was acquired in the coronal plane, n = 48; echo time (TE) = 5.00 msec, repetition time (TR) = 2500 msec, flip angle = 40°, number of excitations (NEX) = 1, image matrix = 256 × 256 mm pixels, 124 continuous slices, slice thickness = 1.5 mm, in-plain resolution = 0.9375 × 0.9375 mm. The MPRAGE was collected using one of three sequences: (1) n = 29, TE = 2.98 msec, TR = 2300 msec, flip angle = 9°, NEX = 1, image matrix = 240 × 256 mm, 160 continuous sagittal slices, slice thickness = 1.2 mm, in-plain resolution = 1 × 1 mm; (2) n = 5; TE = 3.31 msec, TR = 2100 msec, flip angle = 8°, NEX = 1, image matrix = 208 × 256 mm, 176 continuous axial slices, slice thickness = 1 mm, in-plain resolution = 1 × 1 mm; or (3) n = 1; TE = 3.43 msec, TR = 2300 msec, flip angle = 9°, NEX = 1, image matrix = 208 × 256 mm, 176 continuous axial slices, slice thickness = 1 mm, in-plain resolution = 1 × 1 mm. The scanning parameters for one participant's MPRAGE were missing. These structural T1-weighted magnetic resonance images (3D-SPGR or MPRAGE) were AC-PC aligned using Statistical Parametric Mapping (SPM) version 8 (http://www.fil.ion.ucl.ac.uk/spm/software/spm8), then normalized to the International Consortium for Brain Mapping 152 template (Montreal Neurological Institute) via the unified segmentation technique.[73]

Each participant had two FDG-PET studies, one during wakefulness and one during NREM sleep. The FDG injections for PET imaging were conducted at the Sleep and Chronobiology Laboratory during morning wakefulness (2 to 3 h after wake-up time) and during the first NREM sleep cycle. These times were chosen to provide consistent timing across participants, to avoid any effects of sleep inertia, and to capture a period of stable NREM sleep that was unlikely to include REM or wake transitions. Intravenous catheters were placed in each arm of participants: one for the FDG injections and another for venous blood sampling. The FDG injections for the wake PET

scans occurred after 15 to 20 min of continuous wakefulness as participants lay supine in bed with eyes closed. Participants were left undisturbed for 20 min after the injection before being transported by wheelchair to the PET Research Center for the wake PET scan. The FDG injections for the NREM sleep PET scans occurred after 20 min of continuous sleep (NREM stage 2–4) in bed. These injections occurred on average 39 h after the wake FDG injection. Participants were left undisturbed for 20 min before being awakened and transported by wheelchair to the PET center for the NREM sleep PET scan. There were no significant groups differences in injected FDG dose (PI vs. GS) for either the wake or NREM sleep scan, median dose = 6.3 mCi [interquartile range = 6.0, 6.7 mCi] and median dose = 5.5 mCi [interquartile range = 5.4, 7.6 mCi], respectively. Groups did not differ in the amount of time between wake and NREM sleep FDG injections. Sleep-wake states before, during, and 20 min after FDG injections were confirmed using EEG.

Sixty minutes after FDG injection, participants underwent PET imaging using a Siemens/CTI ECAT HR+ tomograph (CTI PET Systems, Knoxville, TN) in 3D mode (63 transaxial planes, FOV = 15.2 cm, slice width = 2.4 mm). Subjects were positioned in the scanner to maximize full brain coverage (cortex through brainstem). A 30 min emission scan (six sequential 5-min scans) was acquired over the 60 to 90 min postinjection period, while participants lay with eyes closed. Venous blood was sampled (1 mL each) at six time points (45, 55, 65, 75, 85, and 90 min postinjection), for the determination of FDG radioactivity (all samples) and glucose (first and last samples) plasma concentrations. A windowed transmission scan (10 to 15 min) was acquired before emission imaging and used for PET attenuation correction. Other corrections included scanner normalization, dead time, scatter, random coincidences, and radioactive decay. The PET data were reconstructed by filtered back-projection. The final in-plane spatial resolution was 6.0 mm. Attenuation-corrected, decay-corrected, FDG-PET data were motion-corrected (if needed) and averaged over all frames (60 to 90 min postinjection) using AIR 3.0 software (http://bishopw.loni.ucla.edu/AIR3/index.html).[74] Each subject's averaged FDG-PET data were coregistered to their AC-PC aligned structural T1-weighted MRI (3D-SPGR or MPRAGE), normalized using the previously obtained transformation parameters, and smoothed with a 10.0 mm full width at half maximum Gaussian filter. Data were quality control checked for FOV positioning, motion, and coregistration problems. Relative regional cerebral metabolic rate for glucose ($rCMR_{glc}$) was calculated at each voxel by dividing the global FDG-PET intensity across all brain voxels for each scan, then multiplying by 50. This calculation accounts for global nuisance effects and puts these relative data into an intuitively accessible scale.

The FDG and glucose plasma concentrations were used to quantify the absolute metabolic rate of deoxyglucose (MRD_{glc}) in the body based on a modified version of a simplified kinetic method,[75] validated and routinely applied in our laboratory.[72] Because the brain metabolizes a large portion of the total glucose utilized in the body, MRD_{glc} provides an indirect, semiquantitative measure of absolute whole-brain glucose metabolism.

Analyses

Assumptions that data were missing at random and normally distributed were checked for each variable. All variables had missing values < 5%. Here, variables with normal distributions, determined using Kolmogorov-Smirnov test for normality, are reported as mean (standard deviation) and variables with non-normal distributions are reported as median [interquartile range]. Demographic and sleep features were compared across groups using Student *t*, Mann-Whitney *U*, or chi-square tests (Tables 1 and 2). Repeated measures analysis of variance was used to examine a group (PI vs. GS) by state (wake vs. NREM sleep) interaction, main effect of group, and main effect of state for MRD_{glc} (semiquantitative estimate of whole-brain metabolism). Aforementioned analyses were conducted in IBM SPSS 22 (IBM Corp., Armonk, NY, USA) or SAS version 9.3 (SAS Institute, Cary, NC).

Relative regional cerebral metabolic rate for glucose ($rCMR_{glc}$) was compared voxelwise across wake and NREM sleep in PI and GS using SPM version 12 (http://www.fil.ion.ucl.ac.uk/spm/software/spm12/). Given the large number of potential brain regions involved in insomnia and their wide distribution, we took a whole-brain voxelwise approach to capture all of these regions in a single analysis, rather than investigating each brain region individually. To correct for multiple comparisons, familywise error (FWE) correction and clusterwise extent thresholds were determined using 3dClustSim (3DC; http://afni.nimh.nih.gov/pub/dist/doc/program_help/3dClustSim.html). Group (PI vs. GS) by state (wake vs. NREM sleep) interactions in $rCMR_{glc}$ were tested using repeated-measures analysis of variance.[76] For this interaction analysis, cluster sizes greater than 249 were significant at height threshold, $P_{uncorrected} < 0.005$; cluster threshold, $P_{3DC\_corrected} < 0.05$; no interactions were significant at the more stringent FWE correction. Main effects for group in $rCMR_{glc}$, averaged voxelwise across wake and NREM sleep states, were tested using an independent samples *t*-test. For this group analysis, cluster sizes greater than 698 were significant at height threshold, $P_{uncorrected} < 0.005$; cluster threshold, $P_{3DC\_corrected} < 0.05$; no group main effects were significant at the more stringent FWE correction. Main effects for state in $rCMR_{glc}$, independent of group, were tested using a paired *t*-test. For this state analysis, cluster sizes greater than 200 were significant at cluster threshold, $P_{FWE\_corrected} < 0.05$. For these main effects analyses, we masked out regions that were significant in the interaction analysis. In Figures 1 through 4, significant clusters were mapped onto brain images in Montreal Neurological Institute space using BrainNet Viewer (https://www.nitrc.org/projects/bnv/).[77] To help interpret the brain images, mean $rCMR_{glc}$ for voxels within selected clusters that showed a significant group-by-state interaction, group main effect, or state main effect were extracted and plotted for each group in each state. We then generated 95% confidence intervals for these clusters using voxelwise data that relied on the voxelwise standard deviation rather than the standard deviation of the mean of the cluster. In the supplemental material (Figures S1 through S3), we also present these same results mapped onto high-resolution structural brain images in xjView (http://www.alivelearn.net/xjview8/). In the supplemental

Table 1—Characteristics of patients with primary insomnia (PI) compared with good sleeper controls (GS).

Characteristic	PI (n = 44)	GS (n = 40)	t / χ^2 / Z	DF	P
Age, y	37 (10)	38 (11)	$t = -0.6$	82	0.585
Sex, female	24 (55%)	25 (63%)	$\chi^2 = 0.6$	1	0.460
Race, White	38 (86%)	31 (78%)	$\chi^2 = 1.1$	1	0.289
Mood symptoms [a]					
Mild-moderate depressive symptoms	18 (42%)	2 (5%)	$\chi^2 = 14.9$	1	< 0.001
Mild-moderate anxiety symptoms	14 (32%)	1 (3%)	$\chi^2 = 9.8$	1	0.002
Pittsburgh Sleep Quality Index, total	12 (3)	2 [1,3]	$Z = -7.9$		< 0.001
Sleep diary					
Sleep onset latency, min	41 (28)	13 (7)	$t = 6.1$	81	< 0.001
Wake-time after sleep onset, min	33 [18,60]	3 [1,9]	$Z = -6.5$		< 0.001
Total sleep time, min	348 (72)	431 (50)	$t = -6.0$	81	< 0.001
Time in bed, min	469 (46)	462 (53)	$t = 0.7$	81	0.335
Sleep efficiency, %	78 [67,82]	93 (3)	$Z = -7.4$		< 0.001
Polysomnography, baseline night					
Sleep onset latency, min	20 [11, 34]	15 [8, 22]	$Z = -1.8$		0.070
Wake-time after sleep onset, min	27 [17, 74]	23 [12, 43]	$Z = -1.6$		0.112
Total sleep time, min	391 [355, 420]	403 (55)	$Z = -1.3$		0.194
Stage 1, min	18 [13, 28]	18 [11, 25]	$Z = -0.9$		0.382
Stage 1, %	5 [3, 7]	4 [3, 6]			
Stage 2, min	242 (48)	250 (41)	$t = -0.8$	82	0.409
Stage 2, %	62 (8)	62 (8)			
Stages 3 and 4, min	20 [7, 48]	23 [8, 59]	$Z = -0.4$		0.697
Stages 3 and 4, %	5 [2, 12]	6 [2, 14]			
REM sleep, min	95 (23)	100 (29)	$t = -0.9$	82	0.363
REM sleep, %	25 (5)	24 (5)			
Time in bed, min	457 (48)	453 (54)	$t = 0.4$	82	0.714
Sleep efficiency, %	89 [78, 92]	93 [86, 94]	$Z = -2.6$		0.008
Apnea-hypopnea index	1 [1, 3]	2 [1, 5]	$Z = -0.9$		0.380
Periodic limb movement arousal index	3 [2, 6]	4 [2, 7]	$Z = -0.3$		0.806

Group values are reported as mean (standard deviation), n (%), or median [interquartile range]. [a] Protocols from which these data were pooled used different instruments for assessing anxiety and depression symptoms. Scores were categorized as minimal or mild-moderate symptoms. Participants did not meet criteria for a current anxiety or depression diagnosis.

material (Figures S4 through S7 and Table S1), we report the results of separate *post hoc* analyses that investigated PI-GS differences in $rCMR_{glc}$ during wake and during NREM sleep considered separately, as well as NREM sleep-wake differences in PI and GS considered separately.

Exploratory Analyses

We sought to confirm that group-by-state interactions in $rCMR_{glc}$ were not driven by the small number of wake epochs that occurred in some participants during the NREM sleep uptake period or the small number of NREM sleep epochs that occurred during the wake uptake period. We conducted a separate exploratory repeated measures analysis of covariance in SPM that adjusted for the number of epochs scored as wake during the morning wake and NREM sleep uptake periods.

We also investigated whether insomnia severity, indexed by sleep efficiency, was related to glucose metabolism. Within PI, regression analyses were used to determine whether sleep efficiency, assessed by daily sleep diary or PSG, was associated with whole-brain MRD_{glc} or $rCMR_{glc}$ during wake or NREM sleep (Figure 4 and Table 6). For the exploratory $rCMR_{glc}$ regression analyses, cluster sizes greater than 222 were significant at height threshold, $P_{uncorrected} < 0.005$; cluster threshold, $P_{3DC\_corrected} < 0.05$); no exploratory $rCMR_{glc}$ regressions were significant at the more stringent FWE correction.

RESULTS

Sleep Features

Table 1 shows sleep characteristics of PI and GS. Patients with PI had significantly higher PSQI scores than GS. On average, PI reported clinically significant symptoms of insomnia on sleep diaries, including > 30 min of unwanted wake time during the night, short sleep duration (< 6 h), and < 80% sleep efficiency. On the baseline night, only PSG-assessed sleep efficiency differed between PI and GS.

On the NREM sleep PET scan night, no group differences were observed for PSG-assessed sleep onset latency, PI = 21

Table 2—Polysomnographic characteristics during the wake and nonrapid eye movement (NREM) sleep [^{18}F]fluoro-2-deoxy-D-glucose positron emission tomography uptake periods in patients with primary insomnia (PI) and good sleeper controls (GS).

Characteristic	PI (n = 44)	GS (n = 40)	Z	P
Wake uptake period				
NREM stages 1–4, min	0.0 [0.0, 0.5]	0.0 [0.0, 0.5]	$Z = -0.4$	0.712
REM, min	0	0	–	–
NREM sleep uptake period [a]				
Wake, min	0.2 [0.0, 0.5]	0.2 [0.0, 0.3]	$Z = -0.1$	0.892
NREM stage 1, min	0.0 [0.0, 1.0]	0.0 [0.0, 0.3]	$Z = -1.1$	0.263
NREM stage 2, min	10.7 (5.8)	13.8 [8.0, 17.0]	$Z = -1.4$	0.173
NREM stages 3–4, min	6.0 [1.3, 12.5]	4.3 [1.3, 8.0]	$Z = -0.7$	0.468

Group values are reported as mean (standard deviation) or median [interquartile range]. [a] In follow-up analyses (data not shown) we investigated whether groups differed in the number of minutes scored as wake during each 5-min block of the 20-min NREM sleep FDG uptake period. Groups did not differ in the amount of wake during the NREM sleep [^{18}F]fluoro-2-deoxy-D-glucose positron emission tomography (FDG-PET) uptake period in any of the 4 blocks ($P > 0.5$, for all). Individuals were excluded from this study for having any REM sleep during the NREM sleep FDG-PET uptake period.

[12, 41] min and GS = 26 (21) min, $Z = -0.5$, P = 0.64. There were no significant group differences in the duration of specific sleep-wake stages during either the wake or NREM sleep uptake periods (Table 2).

Estimated Whole-Brain Glucose Metabolism

There were no significant group-by-state interaction effects, nor significant main effects of group (PI vs. GS) for MRD_{glc}, the semiquantitative estimate of whole-brain glucose metabolism. There was a significant main effect of state (NREM sleep-wake) for MRD_{glc}, which was 18% lower during NREM sleep than wake, NREM sleep = 11.0 (1.7) μmol/100 mL/min, wake = 13.4 (1.9) μmol/100 mL/min, $F_{(1,75)} = 179.5$, $P < 0.001$. Among PI, sleep diary-assessed sleep efficiency was not associated with MRD_{glc} in either wake or NREM sleep. Lower PSG-assessed sleep efficiency was associated with lower wake MRD_{glc}, $r_{(43)} = 0.4$, P = 0.016, but was not associated with NREM sleep MRD_{glc}.

Group-by-State Interactions in Relative Regional Cerebral Metabolic Rate for Glucose

Significant group (PI vs. GS) by state (wake vs. NREM sleep) interactions for $rCMR_{glc}$ were found in clusters located in the right precuneus/posterior cingulate cortex, left middle frontal gyrus, left inferior/superior parietal lobules, left fusiform/lingual/occipital gyri, and, right lingual gyrus, $P_{3DC\_corrected} < 0.05$ for all clusters (Table 3). Significant clusters are shown in the left panel of Figure 1. In the right panel of Figure 1, the extracted mean signal and 95% confidence interval from each cluster are plotted to help interpret the general pattern of interactions. See Figure S1 to view results mapped onto a normalized high-resolution structural MRI. In exploratory analyses, adjusting for the amount of wake during morning wake and NREM sleep did not alter the pattern or level of significance of the interactions.

Significant group-by-state interactions in $rCMR_{glc}$ (relative glucose metabolism) should be interpreted in the context of significantly lower MRD_{glc} (absolute glucose metabolism) during NREM sleep than wake. In this context, higher relative $rCMR_{glc}$ during NREM sleep than wake indicates these clusters had smaller differences in glucose metabolism between wake and NREM sleep than other brain regions. Thus, all group-by-state interactions in $rCMR_{glc}$ should be interpreted as showing a smaller NREM sleep-wake difference in PI than GS in those clusters relative to other brain regions.

Group Differences in Relative Regional Cerebral Metabolic Rate for Glucose, Independent of State

There was a significant main effect of group (PI-GS) for relative $rCMR_{glc}$ across states (Figure 2 and Table 4). Compared with GS, PI had lower $rCMR_{glc}$ in several large clusters including the precuneus/posterior cingulate, anterior cingulate/medial frontal, insula, and temporal cortices. All clusters were significant at $P_{3DC\_corrected} < 0.05$. Significant clusters are shown in the left panel of Figure 2. In the right panel of Figure 2, the extracted mean signal and 95% confidence interval from anatomically distinct regions of the two largest clusters, left precuneus/posterior cingulate and right anterior cingulate (circled in the left panel), were plotted to help interpret the general pattern of the group main effects. See Figure S2 to view results mapped onto a normalized high-resolution structural MRI.

Results for follow-up analyses investigating group differences during wake and during NREM sleep considered separately are reported in Figures S4 and S5, respectively, and Table S1. Visual comparisons of group differences found in only one state should not be used to infer statistically significant state-dependent group differences.

State Differences in Relative Regional Cerebral Metabolic Rate for Glucose, Independent of Group

There was a significant main effect of state (NREM sleep-wake) for relative $rCMR_{glc}$, across groups (Figure 3 and Table 5). Compared with wake, $rCMR_{glc}$ was significantly lower during NREM sleep in large clusters throughout the brain, most notably in the prefrontal cortex. Higher $rCMR_{glc}$ during NREM sleep compared with wake was found in the brainstem, basal ganglia, medial temporal lobe, and motor cortex. Clusters were significant at $P_{FWE\_corrected} < 0.05$. Significant clusters are shown in the left panel of Figure 3. In the right panel of Figure 3, extracted mean signal and 95% confidence interval from anatomically distinct regions of the two largest clusters, right middle frontal gyrus (circled in

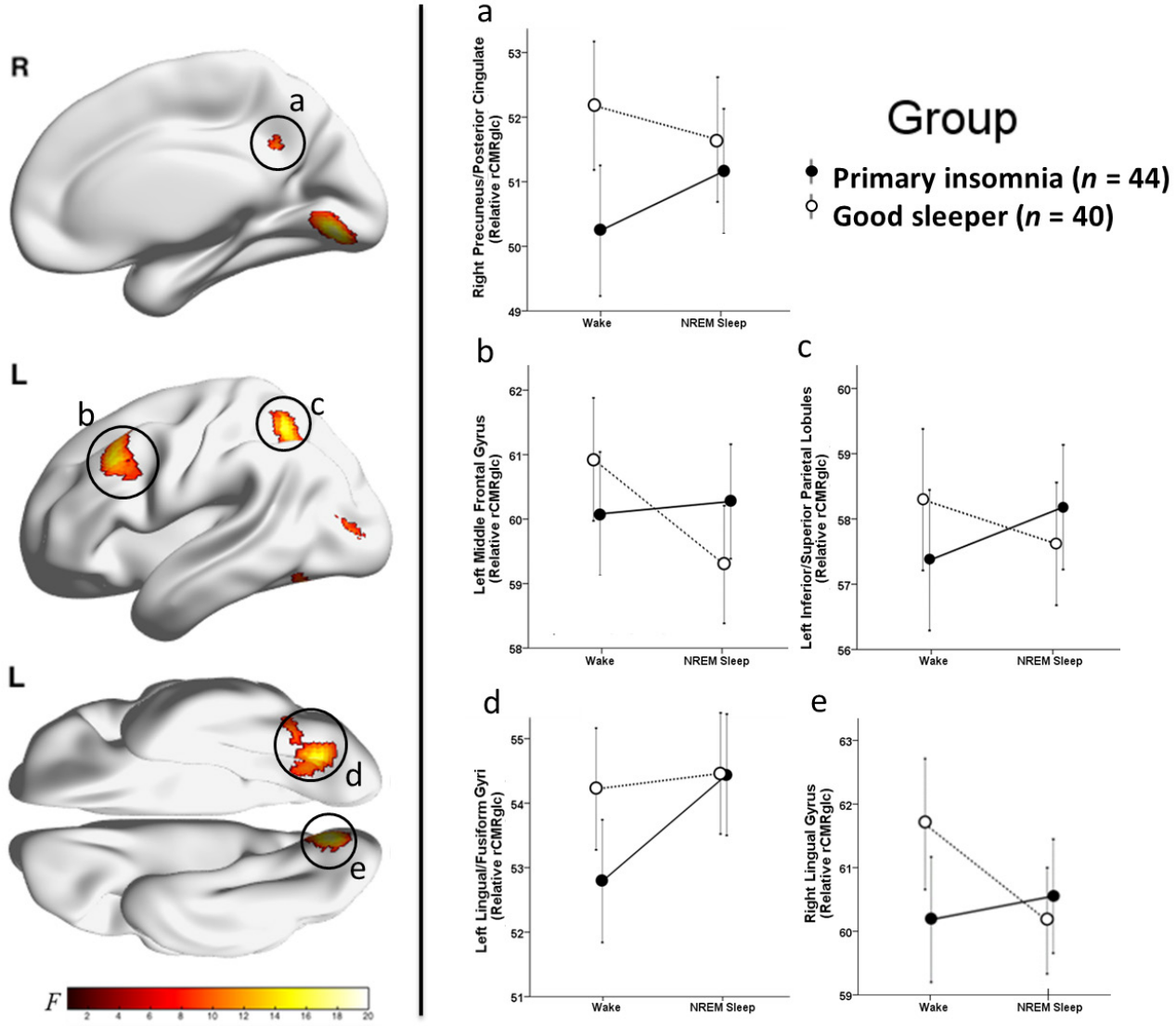

Figure 1—Group-by-state interactions in relative regional cerebral metabolic rate for glucose. We assessed relative regional cerebral metabolic rate for glucose ($rCMR_{glc}$) in a sample of 44 patients with primary insomnia (PI) and 40 good sleeper controls (GS) during wake and nonrapid eye movement (NREM) sleep. Clusters showing significant group (PI vs. GS) by state (wake vs. NREM sleep) interactions for relative $rCMR_{glc}$ are indicated by red-yellow colors in the above brain images. The color bar represents *F* values in the identified clusters. Clusters with significant interactions were identified in regions of the (a) right precuneus/posterior cingulate cortex, (b) left middle frontal gyrus, (c) left inferior/superior parietal lobules, (d) left lingual/fusiform/occipital gyri, and (e) right lingual gyrus, $P_{3DC\_corrected} < 0.05$ for all (Table 3). We extracted the voxelwise data from the circled clusters and plotted these data to the right. In these line graphs, the closed circles connected with a solid line represent extracted average relative $rCMR_{glc}$ from the respective significant cluster (a–e) for PI and the open circles connected by a dotted line represent GS. Error bars represent the 95% confidence interval computed voxelwise within each cluster. L = left; R = right.

Table 3—Group-by-state interactions in relative regional cerebral metabolic rate for glucose.

Cluster[a]	Brain Region	*k*[b]	*F*-statistic (max)	x	y	z
a	Right precuneus and posterior cingulate cortex	307	17.3	22	−56	46
b	Left middle frontal gyrus	349	16.4	−40	22	38
c	Left inferior and superior parietal lobules	391	17.6	−30	−52	54
d	Left lingual, fusiform, middle occipital, and inferior occipital gyri	818	18.6	−26	−72	−14
e	Right lingual gyrus and occipital cortex	315	17.6	8	−78	−6

[a] Clusters a–e correspond to the clusters labeled in Figure 1. [b] Cluster sizes (*k*) greater than 249 were significant at height threshold, $P < 0.005$; cluster threshold, $P_{3DC\_corrected} < 0.05$.

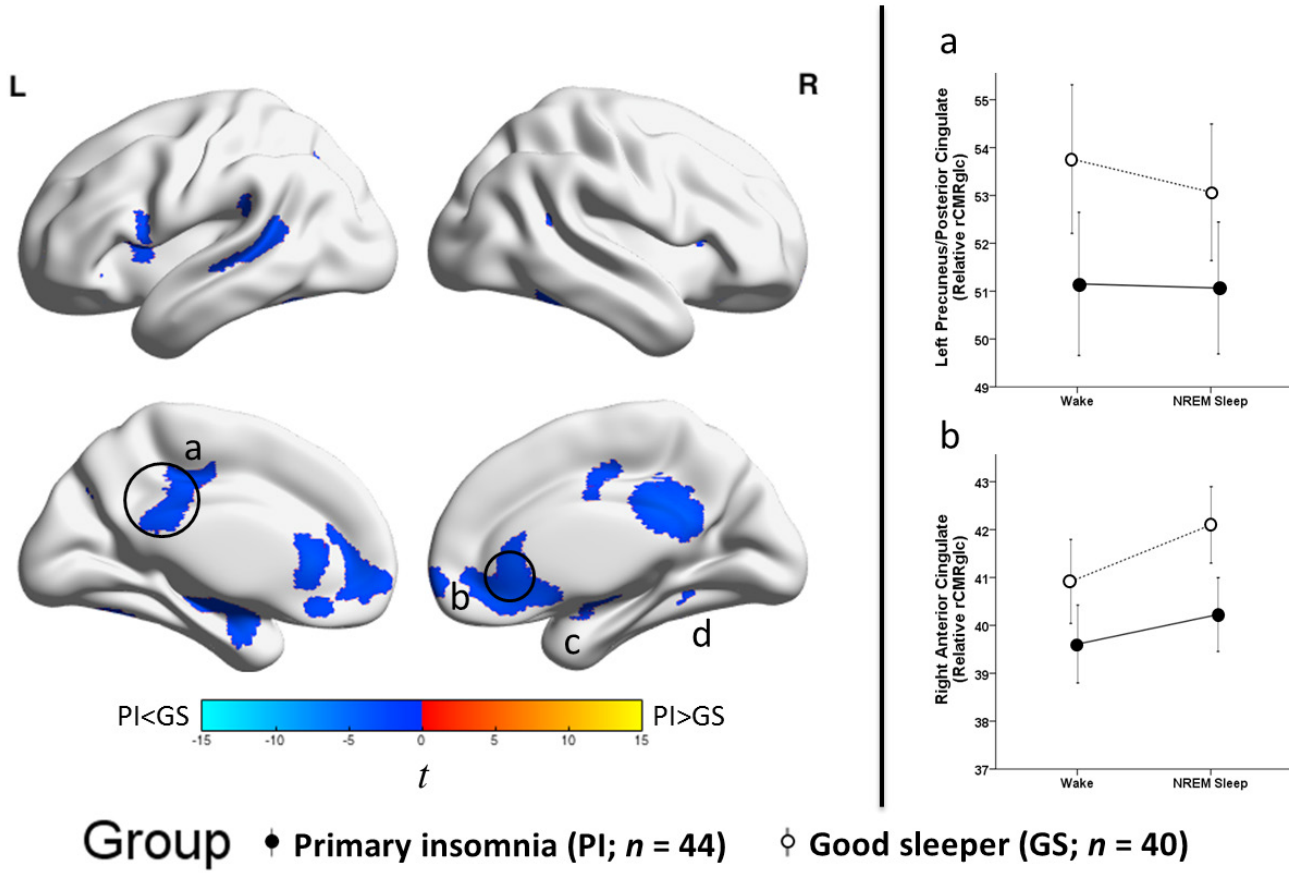

Figure 2—Group differences in relative regional cerebral metabolic rate for glucose, independent of sleep-wake state. We assessed relative regional cerebral metabolic rate for glucose ($rCMR_{glc}$) in a sample of 44 patients with primary insomnia (PI) and 40 good sleeper controls (GS) during wake and nonrapid eye movement (NREM) sleep. To assess group (PI-GS) differences independent of sleep-wake state, we averaged relative $rCMR_{glc}$ values across wake and NREM sleep for each voxel in each participant. The color bar represents *t* values; blue indicates regions where PI had lower relative $rCMR_{glc}$ than GS across wake and NREM sleep, including the (a) bilateral precuneus/posterior cingulate cortex (b) bilateral anterior cingulate/medial frontal cortex, and (c) right hippocampus/amygdala, and (d) right fusiform gyrus, $P_{3DC\_corrected} < 0.05$ for all. A full list of brain regions involving these clusters is presented in Table 4. We extracted the voxelwise data from anatomically distinct regions of the circled clusters, (a) the left precuneus/posterior cingulate and (b) the right anterior cingulate cortex and plotted these data to the right. In these line graphs, the closed circles connected with a solid line represent extracted average $rCMR_{glc}$ from the respective regions for PI, and the open circles connected by a dotted line represent GS. Error bars represent the 95% confidence interval computed voxelwise within each cluster. L = left; R = right.

Table 4—Group differences in relative regional cerebral metabolic rate for glucose ($rCMR_{glc}$), independent of sleep-wake state.

Cluster [a]	Brain Region	*k* [b]	*t*-statistic (max) [c]	x	y	z
a	Bilateral precuneus, posterior cingulate cortex, middle cingulate cortex, superior temporal gyrus, middle temporal gyrus, hippocampus, insula, inferior frontal gyrus, inferior parietal lobe, fusiform gyrus, brainstem, and midbrain	9767	−5.5	12	−40	22
b	Bilateral anterior cingulate, medial frontal gyrus, prefrontal pole, superior frontal, middle frontal, inferior frontal, olfactory gyrus, and caudate	4044	−5.4	12	30	−10
c	Right hippocampus, amygdala, superior temporal gyrus	800	−4.7	36	0	−24
d	Right fusiform gyrus and superior temporal gyrus	762	−3.6	36	−44	16

[a] Clusters a–d correspond to the clusters labeled in Figure 2. [b] Cluster sizes (*k*) greater than 698 voxels were significant at height threshold, $P < 0.005$; cluster threshold, $P_{3DC\_corrected} < 0.05$. [c] Negative *t*-statistics indicate patients with primary insomnia had lower $rCMR_{glc}$ than good sleeper controls.

the left panel) and left brainstem are plotted to help interpret the general pattern of the state main effects. See Figure S3 to view results mapped onto a normalized high-resolution structural MRI.

Significant main effects for state in relative $rCMR_{glc}$ should be interpreted in the context of significantly lower whole-brain metabolic rate for deoxyglucose (MRD_{glc}) during NREM

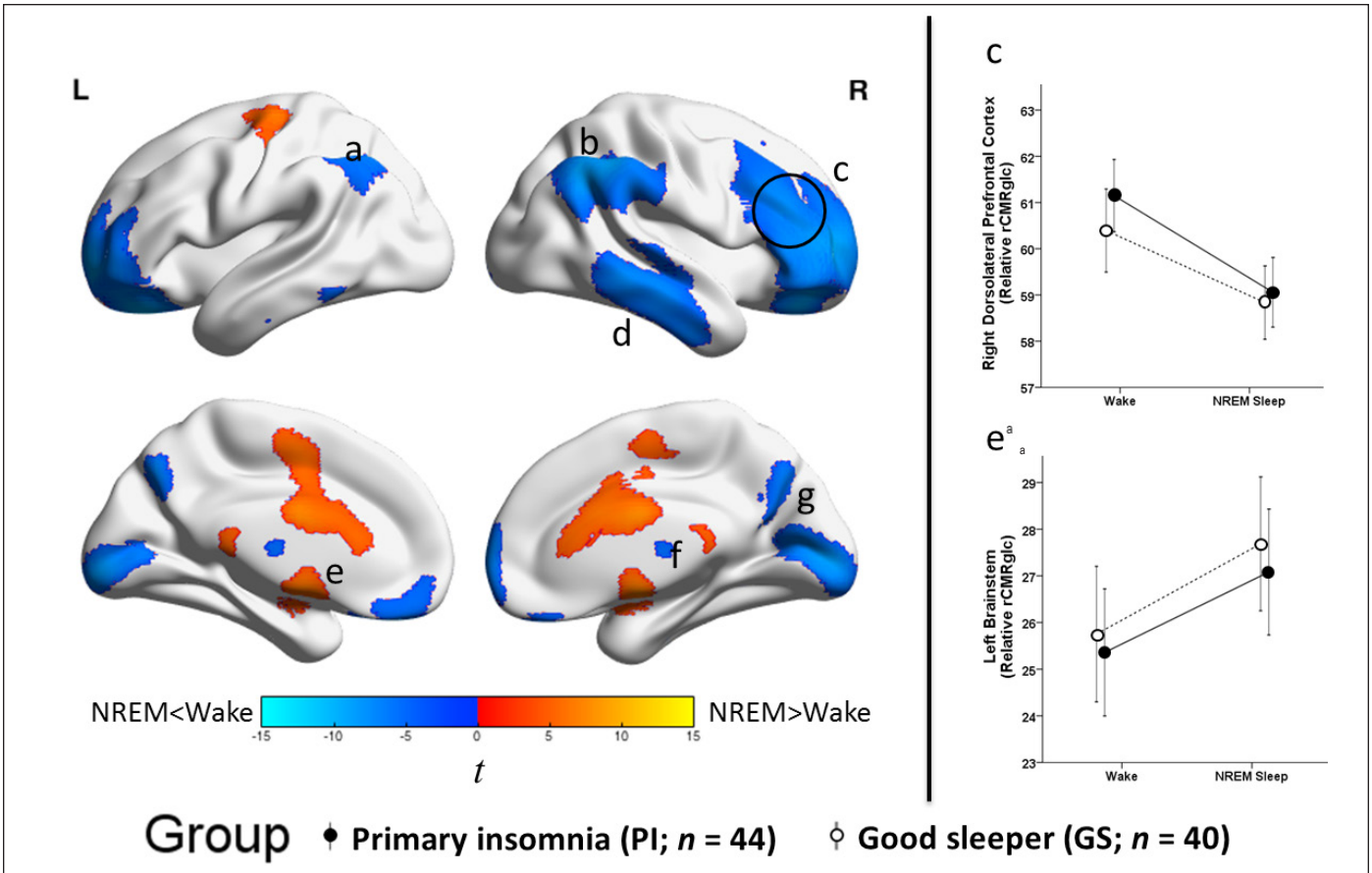

Figure 3—Sleep-wake state differences in relative regional cerebral metabolic rate for glucose, independent of group. We compared relative regional cerebral metabolic rate for glucose ($rCMR_{glc}$) in the total sample, 44 patients with insomnia (PI) and 40 good sleeper controls (GS), during nonrapid eye movement (NREM) sleep to that during wake. The color bar represents *t* values; blue indicates regions where $rCMR_{glc}$ was relatively lower during NREM sleep than wake, and orange indicates regions where $rCMR_{glc}$ was relatively higher during NREM sleep than during wake. Relative $rCMR_{glc}$ was significantly lower during NREM sleep than wake in regions of the (a) left inferior parietal lobule, (b) right inferior parietal lobule, (c) bilateral prefrontal cortex, (d) right temporal cortex, (f) bilateral thalamus, (g) bilateral occipital cortex. Relative $rCMR_{glc}$ was significantly higher during NREM sleep than during wake in regions of the (e) bilateral brainstem/basal ganglia/cingulum/motor areas. All clusters were significant at $P_{FWE\_corrected} < 0.05$. A full list of significant regions is presented in Table 5. We extracted the voxelwise data from anatomically distinct regions of the circled clusters, (c) the right dorsolateral prefrontal cortex and (e) the left brainstem ([a] not depicted), and plotted these data to the right. The closed circles connected with a solid line represent extracted average relative glucose metabolism from the respective regions for PI, and the open circles connected by a dotted line represent GS. Error bars represent the 95% confidence interval computed voxelwise within each cluster. L = left; R = right.

sleep than wake. In other words, regions with higher relative $rCMR_{glc}$ during NREM sleep than wake had the smallest reductions during NREM sleep compared with wake, and regions with significantly lower relative $rCMR_{glc}$ during NREM sleep than wake had the greatest reductions during NREM sleep compared with wake.

Results for follow-up analyses investigating state (NREM sleep-wake) differences in PI and GS considered separately are reported in Figures S6 and S7, respectively, and Table S2 in the supplemental material. Visual comparisons of state differences found in only one group should not be used to infer statistically meaningful group differences.

Insomnia Severity and Relative Regional Cerebral Metabolic Rate for Glucose

Figure 4 displays brain regions showing an association between sleep efficiency, assessed with sleep diary or PSG, and $rCMR_{glc}$ during either wake or NREM sleep. These analyses were conducted in the PI group alone. Lower sleep efficiency measured with sleep diaries was associated with lower relative glucose metabolism during wakefulness in the left insula and with higher relative glucose metabolism during wakefulness in a cluster in the right supramarginal gyrus/postcentral gyri (Figure 4, left panel). Sleep diary-assessed sleep efficiency was not associated with $rCMR_{glc}$ during NREM sleep. During both wake and NREM sleep, lower sleep efficiency measured with PSG on the baseline night was associated with higher relative glucose metabolism in frontal, parietal, occipital, and cerebellar regions (Figure 4, middle and right panels). A full list of brain regions associated with sleep efficiency is presented in Table 6.

DISCUSSION

We found altered patterns of relative glucose metabolism across wake and NREM sleep in brain regions involved in cognition, self-referential processes, and affect among PI compared

Table 5—Sleep-wake state differences in relative regional cerebral metabolic rate for glucose ($rCMR_{glc}$), independent of group.

Cluster [a]	Brain Region	*k* [b]	*t*-statistic (max) [c]	x	y	z
a	Left inferior parietal lobule	632	−7.4	−40	−60	46
b	Right inferior parietal lobule and postcentral gyrus	2333	−9.5	46	−58	40
c	Bilateral prefrontal cortex	8585	−11.2	−16	38	−28
d	Right superior temporal, middle temporal, inferior temporal, and fusiform gyri	1934	−7.5	62	−26	−6
e	Bilateral brainstem, basal ganglia, middle cingulate cortex, postcentral, precentral gyri, supplemental motor area, premotor cortex, anterior cingulate cortex, medial frontal gyrus, middle frontal gyrus, and cerebellum	15355	11.2	12	−14	−40
f	Bilateral thalamus	99	−5.7	4	−14	8
*	Right precuneus	318	7.5	2	−70	68
g	Bilateral occipital cortex, lingual gyrus, precuneus, posterior cingulate cortex, and superior parietal lobule	3359	−8.6	8	−90	2
*	Right hippocampus and amygdala	227	7	28	6	−12
*	Left cerebellum	2541	−9.6	−44	−64	−40
*	Right cerebellum	3281	−11.5	30	−74	−44

[a] Clusters a–g correspond to the clusters labeled in Figure 3. Clusters with an * were significant but are not labeled in Figure 3. [b] Cluster sizes (*k*) greater than 200 voxels were significant at height threshold, $P_{FWE\_corrected} < 0.05$. The cluster in the thalamus was smaller than 200 voxels but was significant at $P_{FWE\_corrected} < 0.05$. [c] Negative *t*-statistics indicate that $rCMR_{glc}$ was lower during nonrapid eye movement (NREM) sleep than wake; positive *t*-statistics indicate that $rCMR_{glc}$ was greater during NREM sleep than during wake. Sleep-wake state differences should be interpreted in the context of a global reduction in glucose metabolism during NREM sleep compared with wake. Thus, positive *t*-statistics indicate regions that had the least NREM sleep-wake differences in glucose metabolism and negative *t*-statistics indicate regions with the greatest NREM sleep-wake differences.

to GS. However, we did not find evidence for altered NREM sleep-wake differences in relative glucose metabolism in brain regions typically discussed as wake-promoting centers (i.e., brainstem). Consistent with several previous PET studies in good sleepers, the greatest NREM sleep-wake differences for both groups were observed in the prefrontal cortex, parietal cortex, and cerebellum. As found in a prior study that used the FDG PET method,[29] higher relative glucose metabolism during NREM sleep than wake was observed in several regions, including the brainstem. In contrast, prior studies that used the $H_2{}^{15}O$ PET method consistently showed lower blood flow in the brainstem during NREM sleep than wake.[19,20,22] Differences across studies may be due to methodology, such as the PET method used (i.e., $H_2{}^{15}O$, which measures blood flow vs. ^{18}F-FDG, which measures regional glucose metabolism); the sleep environment (i.e., scanner in many previous studies vs. bed for the current study); and the use of sleep deprivation prior to scanning, which has been used in several previous studies, but not in the current study. In the current study, both groups had significantly lower whole-brain glucose metabolism during NREM sleep than during wake. Therefore, regions with higher relative glucose metabolism during NREM sleep than wake should be interpreted as having smaller sleep-wake differences. Moreover, interactions in which PI had higher relative glucose metabolism during NREM sleep than wake, compared with GS, should be interpreted as PI having smaller NREM sleep-wake differences than GS. All interactions suggest that PI had a smaller decline than GS during NREM sleep compared with wake or, equivalently, a smaller increase during wake compared with NREM sleep in these clusters. Our findings build on the growing number of neuroimaging studies suggesting that insomnia is a neurobiologically complex disorder characterized by regional alterations in brain activity across wake and NREM sleep. The median PSG sleep efficiency of the PI group was 89%, which indicates that a large number of patients lacked objective markers of insomnia on the baseline night; thus, these findings may not generalize to all insomnia subtypes, including those with more objectively severe insomnia. It is also worth noting that we used a stringent definition of sleep efficiency, with the denominator including only time between lights out and final awakening, and that all participants slept at habitual sleep-wake times, rather than a fixed 8-h interval. Although causal inferences cannot be made with these data, our findings may help elucidate the pathophysiological mechanisms and neurobehavioral consequences of chronic insomnia.

Pathophysiology of Insomnia

Differences in relative glucose metabolism between PI and GS may provide new insights regarding the pathophysiology of insomnia, within the framework of "hyperarousal" and other neurobiological models. Hyperarousal is a loosely-defined construct that denotes heightened cognitive, cortical, affective, or central nervous system activity that disrupts sleep and causes daytime impairments.[78] In the context of the current and previous[33] FDG-PET studies, hyperarousal may be inferred from smaller NREM sleep-wake differences in regional brain metabolism among PI compared with GS (i.e., group-state interactions). We found such interactions in the precuneus/posterior cingulate cortex, left middle frontal gyrus, left

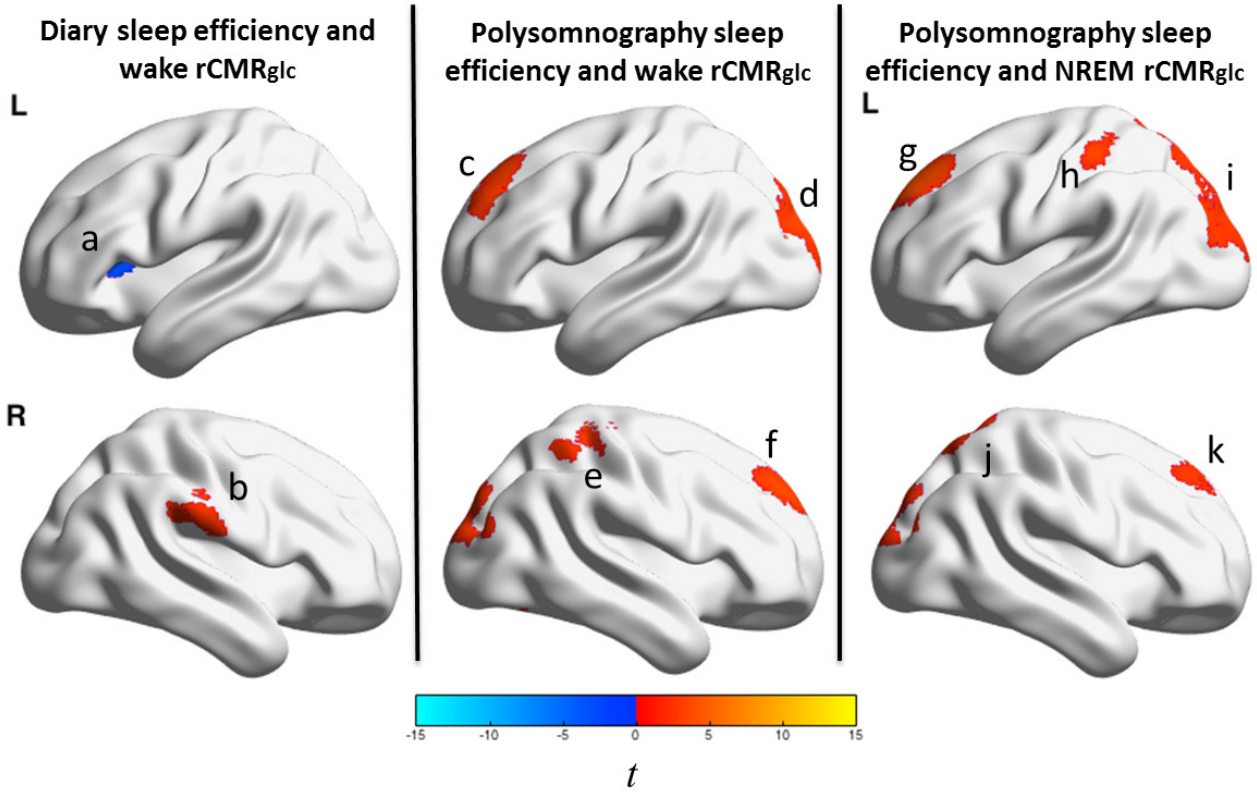

Figure 4—Sleep efficiency and relative regional cerebral metabolic rate for glucose in patients with insomnia. We tested associations between sleep efficiency (sleep diary and polysomnography assessed) and relative regional cerebral metabolic rate for glucose ($rCMR_{glc}$) during wake and nonrapid eye movement (NREM) sleep in a sample of 44 patients with primary insomnia (PI). The color bar represents *t* values; orange indicates regions where sleep efficiency negatively correlated with relative $rCMR_{glc}$ and blue indicates regions where there was a positive correlation. Lower sleep diary-assessed sleep efficiency was associated with (a) lower relative $rCMR_{glc}$ during wakefulness in the left anterior insula and (b) higher relative $rCMR_{glc}$ during wakefulness in the right supramarginal gyrus (left panel). Sleep diary-assessed sleep efficiency was not associated with relative $rCMR_{glc}$ during NREM sleep. Lower polysomnography-assessed sleep efficiency was associated with higher relative $rCMR_{glc}$ during wakefulness in regions of the (c) left superior frontal gyrus, (d) occipital gyri, (e) right inferior parietal lobule/postcentral/precentral gyri, and (f) right superior frontal/medial frontal gyri (middle panel). Lower polysomnography-assessed sleep efficiency was associated with higher relative $rCMR_{glc}$ during NREM sleep in regions of the (g) left superior frontal/medial frontal gyri, (h) left postcentral gyrus, (i) bilateral superior parietal lobule/occipital gyri, (j) right superior parietal lobule/postcentral/precuneus gyri, and (k) right superior frontal/medial frontal gyri (middle panel). All clusters were significant at $P_{3DC\_corrected} < 0.05$. A full list of significant clusters and brain regions involving these clusters is presented in Table 6. L = left; R = right.

inferior/superior parietal lobules, and lingual/fusiform/occipital gyri. Smaller NREM sleep-wake differences in metabolic rate in these regions may reflect relatively greater metabolic rate during NREM sleep, and therefore, could be consistent with a state-specific hyperarousal.

Hyperarousal may also be inferred from stable PI-GS differences in regional brain metabolism across both wake and NREM sleep, i.e., main effects of group. Our findings in this regard are less consistent with the predictions of the hyperarousal model. Irrespective of state, PI had lower relative glucose metabolism in regions of the precuneus/posterior cingulate, parietal lobe, medial prefrontal, anterior cingulate, and temporal regions, brain regions plausibly related to the cognitive-affective symptoms of insomnia. Nevertheless, these brain regions are also involved in the default mode network, a network that is activated during quiet wakefulness compared with task engagement, and for which lower glucose metabolism during morning wakefulness may reflect hyperarousal. Hyperarousal may also be indicated by an association between higher glucose metabolism and more severe insomnia symptoms. Sleep diary-assessed sleep efficiency was inversely related to relative glucose metabolism in the right supramarginal gyrus. Moreover, PSG-assessed sleep efficiency was inversely related to relative glucose metabolism in several frontal and parietal regions during both wake and NREM states, which may be seen as consistent with the hyperarousal hypothesis. However, several findings are less consistent with a general hyperarousal model of insomnia: sleep diary-assessed sleep efficiency was not associated with relative glucose metabolism during NREM sleep; lower sleep diary-assessed sleep efficiency among PI was associated with lower relative glucose metabolism in the left insula during wakefulness; lower PSG-assessed sleep efficiency among PI was associated with lower whole-brain glucose during wakefulness; and lower PSG-assessed sleep efficiency was not related to whole-brain glucose metabolism during NREM sleep.

Our findings may also be interpreted in the context of other sleep-wake regulatory processes that contribute to the

Table 6—Sleep efficiency and relative regional cerebral metabolic rate for glucose ($rCMR_{glc}$) in patients with insomnia.

Analysis	Cluster [a]	Brain Region	*k* [b]	*t*-statistic (max) [c]	x	y	z
Diary sleep efficiency × wake $rCMR_{glc}$	a	Left insula	369	4.3	−30	22	10
	*	Right insula	279	−3.7	28	−28	18
	b	Right supramarginal and postcentral gyri	424	−3.5	54	−32	32
	*	Left cerebellum	1232	−4	−4	−84	−34
Diary sleep efficiency × NREM $rCMR_{glc}$	N/A	None	N/A	N/A	N/A	N/A	N/A
Polysomnography sleep efficiency × wake $rCMR_{glc}$	c	Left superior frontal gyrus	328	−3.8	−18	38	46
	d	Bilateral superior occipital, middle occipital, precuneus, cuneus gyri	2442	−4.1	−14	−98	22
	e	Right inferior parietal lobule and postcentral and precentral gyri	572	−4.4	28	−36	60
	f	Right superior frontal and medial frontal gyri	439	−4.1	18	48	36
	*	Left cerebellum and lingual gyrus	907	−3.3	−38	−78	−22
	*	Right rectal gyrus	309	−3.7	0	24	−24
	*	Right cerebellum	606	−3.4	20	−92	−32
	*	Right cerebellum	324	−3.5	30	−42	−52
Polysomnography sleep efficiency × NREM $rCMR_{glc}$	g	Left superior frontal and medial frontal gyri	718	−5.2	−14	46	42
	h	Left postcentral gyrus	314	−3.8	−40	−32	54
	i	Bilateral superior parietal lobule and precuneus, cuneus, and middle occipital gyri	3062	−3.9	8	−96	22
	j	Right superior parietal lobule and postcentral and precuneus gyri	571	−3.7	22	−70	64
	k	Right superior frontal and middle frontal gyri	255	−3.8	24	38	44

[a] Clusters a–k correspond to the clusters labeled in Figure 4. Clusters with an * were significant but are not labeled in Figure 4. [b] Cluster sizes (*k*) greater than 222 voxels were significant at height threshold, $P < 0.005$; cluster threshold, $P_{3DC\_corrected} < 0.05$. [c] Negative *t*-statistics indicate negative correlations and positive *t*-statistics indicate positive correlations. NREM, nonrapid eye movement.

pathophysiology of insomnia. For instance, it is plausible to hypothesize that brain regions involved in cognitive, self-referential, and affective processes show altered patterns of inhibition during NREM sleep among individuals with insomnia. Altered inhibition during NREM sleep could result in a lack of regionally restorative sleep (i.e., reduced regional sleep intensity, or a type of "localized sleep deprivation"), and ultimately, to daytime impairments in the functions subserved by these regions. Alternatively, reduced engagement of specific brain regions during wakefulness could lead to reduced use-dependent sleep intensity in those regions during NREM sleep, and hence to relative glucose metabolism during NREM sleep that is equivalent to or higher than that during wake. The significant group-by-state interactions identified in this study clustered in brain regions whose activation/deactivation is associated with homeostatic sleep drive (i.e., left frontal cortex) and consciousness (i.e., precuneus/posterior cingulate). This explanation is consistent with other observations regarding use-dependent increases in local sleep intensity.[79] The finding that PI had lower glucose metabolism than GS during both wake and NREM sleep may reflect a state independent alterations as well. A recent study found that insomnia was associated with impaired structural connectivity in the default mode network, a network that has lower anterior-posterior connectivity during the sleep-wake transition.[42] Thus, insomnia may also involve state-independent alterations in brain circuitry that characterizes sleep-wake states.

These proposed mechanisms are not mutually exclusive. Regardless of whether one interprets these findings from the perspective of hyperarousal, impaired inhibition, use-dependent sleep intensity, and/or impaired network connectivity that characterizes sleep-wake states, our findings strongly suggest that the pathophysiology of insomnia should be conceptualized as a set of regional alterations in brain function, rather than as a global brain phenomenon.

Neurobehavioral Consequences of Insomnia

We found that PI differed from GS in terms of relative glucose metabolism across wake and NREM sleep in several brain regions involved in cognitive, self-referential, and affective brain processes. The left middle frontal gyrus and left parietal cortex are major nodes of the executive control network, which is involved in executive function broadly, attention, working memory, and episodic memory.[80,81] The fusiform/lingual/occipital gyri are involved in the perceptual processing of faces and emotional expressions, naming, and self-referential processing associated with self-appraisal and self-criticism (e.g., rumination).[15,16,82,83] The posterior cingulate cortex and adjacent

precuneus are central nodes of the default mode network that is involved in mind-wandering, consciousness, episodic memory retrieval, and integrating cognitive and affective information in relation to self.[84,85] Functional abnormalities in the precuneus/posterior cingulate cortex, left hemisphere (including frontoparietal regions),[86] and fusiform/lingual gyri[18,87] have been linked to depression.[86,88] Insomnia has been associated with mild impairments in problem-solving, working memory, episodic memory, rumination, and facial processing.[6,8,89] and prospectively predicts the onset and severity of depressive syndromes.[9] Collectively, dysfunction in the brain regions identified in this study may correspond to the cognitive, self-referential, and affective difficulties often experienced by PI. Regions identified in this study as showing altered NREM sleep-wake differences in PI compared with GS may be fruitful treatment targets for mitigating negative outcomes of insomnia.

Clinical Implications

Group and group-by-state differences in relative glucose metabolism occurred in the absence of clinically significant group differences in PSG-measured sleep. Insomnia disorder is diagnosed by self-report, and may reflect a state- and brain region-specific sleep disturbance experienced by patients and inadequately captured by objective measures of sleep that characterize sleep as a global state (e.g., PSG or actigraphy). Although insomnia diagnosis was generally associated with relative regional hypometabolism during wake and NREM sleep, our PSG indicator of poor sleep in PI was associated with relative regional hypermetabolism during wake and NREM sleep. Interestingly, our sleep diary indicator of poor sleep in PI was only associated with relative glucose metabolism during wakefulness (i.e., lower relative $rCMR_{glc}$ in the left anterior insula and higher relative $rCMR_{glc}$ in the right supramarginal gyrus). Thus, self-reported severity of sleep symptoms, above and beyond insomnia diagnosis, may relate more to functional brain alterations that occur during wakefulness than during NREM sleep. Future studies should address how self-reported and PSG-measured sleep features relate to regional measures of brain function during sleep and wakefulness as this may help identify evidence-based insomnia subtypes.

Although evidence-based treatments for insomnia are well developed,[90,91] their mechanisms of action remain poorly understood. Studies examining regional brain function and brain metabolism may help elucidate treatment effects. For instance, treatments capable of more specifically targeting regional brain dysregulation in insomnia, such as cognitive training,[7] mindfulness meditation,[92] or repetitive transcranial magnetic stimulation,[93] may help to augment treatment efficacy. The left middle frontal gyrus, left inferior/superior parietal lobules, lingual/fusiform gyri, and precuneus/posterior cingulate cortex—as well as the brain networks they subserve—may represent meaningful targets for such interventions.

Strengths and Limitations

This study has several strengths, including the largest sample to date of FDG-PET imaging in insomnia patients, and well-characterized study samples. Our sample is much larger than that in the preliminary FDG-PET study of insomnia from our group,[33] and insomnia is a heterogeneous condition, which may account for discrepant findings across these two analyses. Using the FDG-PET method allows participants to sleep, without sleep deprivation, in a typical sleep laboratory bed during uptake and later be awakened for scanning. Thus, the functional patterns obtained from the FDG-PET method reflect NREM sleep occurring at a typical time, and after a typical duration of wakefulness for each individual.

The main limitation of the FDG-PET methodology is the necessity of injecting a radioactive tracer, which may cause awakenings. Nevertheless, the success rate for NREM sleep PET scans in this study (81%) was within the range achieved in previous PET sleep studies (range 31–93%).[26,27,94,95]

Other potential limitations relate to the study method and sample. Because the PET data result from sleep collected in the laboratory, findings may not generalize to sleep in patients' typical sleep environment assessed over a longer period of time. Moreover, the cross-sectional design of this study did not allow us to differentiate whether the brain regions identified are causally related to the pathophysiology of insomnia, its onset or maintenance, or the negative consequences of insomnia. Our sample included individuals with PI diagnosed by clinical criteria, and the results may not generalize to patients with comorbid conditions or more severe objective sleep disturbance. Although none of the PI participants had a currently diagnosed depression or anxiety disorder, they did have relatively elevated symptoms compared with GS, and our findings could in part reflect these symptoms.

CONCLUSIONS

These findings support the conceptualization of insomnia as a regionally specific and state-dependent sleep disorder involving brain regions related to cognitive, self-referential, and affective processes. Structural and functional abnormalities in the precuneus/posterior cingulate cortex,[48] left frontal cortex,[33,48] left parietal cortex,[33,44] and left fusiform gyrus[47] have been linked to insomnia using other types of neuroimaging methods (i.e., MRI, functional MRI, SPECT, PET). Brain region-specific differences were found in the absence of group (PI vs. GS) differences in global FDG uptake. We propose that group (PI vs. GS) by state (wake vs. NREM sleep) interactions in relative glucose metabolism may be explained by either reduced activation of these brain regions during wake or reduced deactivation during NREM sleep. This pattern may provide clues to the pathophysiological of insomnia and its neurophysiological consequences. Future studies investigating the neurobiology of insomnia may benefit from additional neuroimaging studies capable of capturing both temporal and spatial dimensions of insomnia pathophysiology that align with our current understanding of sleep neurobiology.[96] These findings may also stimulate the search for novel models of insomnia and treatments that target the neurobiological basis of insomnia and its consequences.

REFERENCES

1. American Academy of Sleep Medicine. International Classification of Sleep Disorders, 3rd ed. Westchester, IL: American Academy of Sleep Medicine, 2014.

2. American Psychiatric Association. Diagnostic and Statistical Manual of Mental Disorders, 5th ed. Arlington, VA: American Psychiatric Association, 2013.
3. Chung KF, Yeung WF, Ho FY, Yung KP, Yu YM, Kwok CW. Cross-cultural and comparative epidemiology of insomnia: the Diagnostic and Statistical Manual (DSM), International Classification of Diseases (ICD) and International Classification of Sleep Disorders (ICSD). Sleep Med 2015;16:477–82.
4. Léger D, Bayon V. Societal costs of insomnia. Sleep Med Rev 2010;14:379–89.
5. Parthasarathy S, Vasquez MM, Halonen M, et al. Persistent insomnia is associated with mortality risk. Am J Med 2015;128:268–75.
6. Fortier-Brochu E, Beaulieu-Bonneau S, Ivers H, Morin CM. Insomnia and daytime cognitive performance: a meta-analysis. Sleep Med Rev 2012;16:83–94.
7. Haimov I, Shatil E. Cognitive training improves sleep quality and cognitive function among older adults with insomnia. PLoS One 2013;8:e61390.
8. Vincent NK, Walker JR. Perfectionism and chronic insomnia. J Psychosom Res 2000;49:349–54.
9. Baglioni C, Battagliese G, Feige B, et al. Insomnia as a predictor of depression: a meta-analytic evaluation of longitudinal epidemiological studies. J Affect Disord 2011;135:10–9.
10. Schmidt RE, Harvey AG, Van der Linden M. Cognitive and affective control in insomnia. Front Psychol 2011;2:349.
11. Andrews-Hanna JR, Saxe R, Yarkoni T. Contributions of episodic retrieval and mentalizing to autobiographical thought: evidence from functional neuroimaging, resting-state connectivity, and fMRI meta-analyses. Neuroimage 2014;91:324–35.
12. Wager TD, Smith EE. Neuroimaging studies of working memory: a meta-analysis. Cogn Affect Behav Neurosci 2003;3:255–74.
13. Unterrainer JM, Rahm B, Kaller CP, et al. When planning fails: individual differences and error-related brain activity in problem solving. Cereb Cortex 2004;14:1390–7.
14. DeLeon J, Gottesman RF, Kleinman JT, et al. Neural regions essential for distinct cognitive processes underlying picture naming. Brain 2007;130:1408–22.
15. Brühl AB, Rufer M, Kaffenberger T, Baur V, Herwig U. Neural circuits associated with positive and negative self-appraisal. Neuroscience 2014;265:48–59.
16. Longe O, Maratos FA, Gilbert P, et al. Having a word with yourself: neural correlates of self-criticism and self-reassurance. Neuroimage 2010;49:1849–56.
17. Sundermann B, Olde Lutke BM, Pfleiderer B. Toward literature-based feature selection for diagnostic classification: a meta-analysis of resting-state fMRI in depression. Front Hum Neurosci 2014;8:692.
18. Groenewold NA, Opmeer EM, de JP, Aleman A, Costafreda SG. Emotional valence modulates brain functional abnormalities in depression: evidence from a meta-analysis of fMRI studies. Neurosci Biobehav Rev 2013;37:152–63.
19. Braun AR, Balkin TJ, Wesenten NJ, et al. Regional cerebral blood flow throughout the sleep-wake cycle. An H215O PET study. Brain 1997;120:1173–97.
20. Hofle N, Paus T, Reutens D, et al. Regional cerebral blood flow changes as a function of delta and spindle activity during slow wave sleep in humans. J Neurosci 1997;17:4800–8.
21. Andersson JL, Onoe H, Hetta J, et al. Brain networks affected by synchronized sleep visualized by positron emission tomography. J Cereb Blood Flow Metab 1998;18:701–15.
22. Kajimura N, Uchiyama M, Takayama Y, et al. Activity of midbrain reticular formation and neocortex during the progression of human non-rapid eye movement sleep. J Neurosci 1999;19:10065–73.
23. Finelli LA, Landolt HP, Buck A, et al. Functional neuroanatomy of human sleep states after zolpidem and placebo: a H215O-PET study. J Sleep Res 2000;9:161–73.
24. Dang-Vu TT, Desseilles M, Laureys S, et al. Cerebral correlates of delta waves during non-REM sleep revisited. Neuroimage 2005;28:14–21.
25. Hiroki M, Uema T, Kajimura N, et al. Cerebral white matter blood flow is constant during human non-rapid eye movement sleep: a positron emission tomographic study. J Appl Physiol 2005;98:1846–54.
26. Maquet P, Dive D, Salmon E, et al. Cerebral glucose utilization during sleep-wake cycle in man determined by positron emission tomography and [18F]2-fluoro-2-deoxy-D-glucose method. Brain Res 1990;513:136–43.
27. Maquet P, Dive D, Salmon E, et al. Cerebral glucose utilization during stage 2 sleep in man. Brain Res 1992;571:149–53.
28. Buchsbaum MS, Hazlett EA, Wu J, Bunney WE, Jr. Positron emission tomography with deoxyglucose-F18 imaging of sleep. Neuropsychopharmacology 2001;25:S50–6.
29. Nofzinger EA, Buysse DJ, Miewald JM, et al. Human regional cerebral glucose metabolism during non-rapid eye movement sleep in relation to waking. Brain 2002;125:1105–15.
30. Maquet P, Degueldre C, Delfiore G, et al. Functional neuroanatomy of human slow wave sleep. J Neurosci 1997;17:2807–12.
31. Cano G, Mochizuki T, Saper CB. Neural circuitry of stress-induced insomnia in rats. J Neurosci 2008;28:10167–84.
32. Buysse DJ, Germain A, Hall M, Monk TH, Nofzinger EA. A neurobiological model of insomnia. Drug Discov Today Dis Models 2011;8:129–37.
33. Nofzinger EA, Buysse DJ, Germain A, Price JC, Miewald JM, Kupfer DJ. Functional neuroimaging evidence for hyperarousal in insomnia. Am J Psychiatry 2004;161:2126–9.
34. Riemann D, Voderholzer U, Spiegelhalder K, et al. Chronic insomnia and MRI-measured hippocampal volumes: a pilot study. Sleep 2007;30:955–8.
35. Altena E, Vrenken H, Van Der Werf YD, van den Heuvel OA, Van Someren EJ. Reduced orbitofrontal and parietal gray matter in chronic insomnia: a voxel-based morphometric study. Biol Psychiatry 2010;67:182–5.
36. Winkelman JW, Benson KL, Buxton OM, et al. Lack of hippocampal volume differences in primary insomnia and good sleeper controls: an MRI volumetric study at 3 Tesla. Sleep Med 2010;11:576–82.
37. Winkelman JW, Plante DT, Schoerning L, et al. Increased rostral anterior cingulate cortex volume in chronic primary insomnia. Sleep 2013;36:991–8.
38. Noh HJ, Joo EY, Kim ST, et al. The relationship between hippocampal volume and cognition in patients with chronic primary insomnia. J Clin Neurol 2012;8:130–8.
39. Joo EY, Noh HJ, Kim JS, et al. Brain gray matter deficits in patients with chronic primary insomnia. Sleep 2013;36:999–1007.
40. Joo EY, Kim H, Suh S, Hong SB. Hippocampal substructural vulnerability to sleep disturbance and cognitive impairment in patients with chronic primary insomnia: magnetic resonance imaging morphometry. Sleep 2014;37:1189–98.
41. Spiegelhalder K, Regen W, Baglioni C, et al. Insomnia does not appear to be associated with substantial structural brain changes. Sleep 2013;36:731–7.
42. Suh S, Kim H, Dang-Vu TT, Joo E, Shin C. Cortical thinning and altered cortico-cortical structural covariance of the default mode network in patients with persistent insomnia symptoms. Sleep 2016;39:161–71.
43. Corsi-Cabrera M, Figueredo-Rodríguez P, del Río-Portilla Y, Sánchez-Romero J, Galán L, Bosch-Bayard J. Enhanced frontoparietal synchronized activation during the wake-sleep transition in patients with primary insomnia. Sleep 2012;35:501–11.
44. Smith MT, Perlis ML, Chengazi VU, et al. Neuroimaging of NREM sleep in primary insomnia: a Tc-99-HMPAO single photon emission computed tomography study. Sleep 2002;25:325–35.
45. Huang Z, Liang P, Jia X, et al. Abnormal amygdala connectivity in patients with primary insomnia: evidence from resting state fMRI. Eur J Radiol 2012;81:1288–95.

46. Chen MC, Chang C, Glover GH, Gotlib IH. Increased insula coactivation with salience networks in insomnia. Biol Psychol 2014;97:1–8.
47. Dai XJ, Peng DC, Gong HH, et al. Altered intrinsic regional brain spontaneous activity and subjective sleep quality in patients with chronic primary insomnia: a resting-state fMRI study. Neuropsychiatr Dis Treat 2014;10:2163–75.
48. Li Y, Wang E, Zhang H, et al. Functional connectivity changes between parietal and prefrontal cortices in primary insomnia patients: evidence from resting-state fMRI. Eur J Med Res 2014;19:32.
49. Nie X, Shao Y, Liu SY, et al. Functional connectivity of paired default mode network subregions in primary insomnia. Neuropsychiatr Dis Treat 2015;11:3085–93.
50. American Psychiatric Association. Diagnostic and statistical manual of mental disorders, 4th ed., Text Revision. Arlington, VA: American Psychiatric Association, 2000.
51. Nofzinger EA, Mintun MA, Price J, et al. A method for the assessment of the functional neuroanatomy of human sleep using FDG PET. Brain Res Protoc 1998;2:191–8.
52. First M, Spitzer RL, Gibbon M, Williams JBW. Structured Clinical Interview for DSM-IV Axis I Disorders-Patient Edition (SCID-I/P). Version 2.0. New York, NY: New York State Psychiatric Institute, 1995.
53. Beck AT, Epstein N, Brown G, Steer RA. An inventory for measuring clinical anxiety: psychometric properties. J Consult Clin Psychol 1988;56:893–7.
54. Spielberger CD, Gorsuch RL, Luschene RE. Manual for the State-Trait Anxiety Inventory. Palo Alto, CA: Consulting Psychologists Press, 1970.
55. Beck AT, Ward CH, Mendelson M, Mock J, Erbaugh J. An inventory for measuring depression. Arch Gen Psychiatry 1961;4:561–71.
56. Rush AJ, Giles DE, Schlesser MA, Fulton CL, Weissenburger J, Burns C. The Inventory for Depressive Symptomatology (IDS): preliminary findings. Psychiatry Res 1986;18:65–87.
57. Rush AJ, Gullion CM, Basco MR, Jarrett RB, Trivedi MH. The Inventory of Depressive Symptomatology (IDS): psychometric properties. Psychol Med 1996;26:477–86.
58. McNair DM, Lorr M, Droppleman LF. Manual for the Profile of Mood States. San Diego, CA: Educational and Industrial Testing Service, 1971.
59. Rush AJ, Trivedi MH, Ibrahim HM, et al. The 16-Item Quick Inventory of Depressive Symptomatology (QIDS), clinician rating (QIDS-C), and self-report (QIDS-SR): a psychometric evaluation in patients with chronic major depression. Biol Psychiatry 2003;54:573–83.
60. Beck A, Steer R, Garbin M. Psychometric properties of the Beck Depression Inventory: twenty-five years of evaluation. Clin Psychol Rev 1988;8:77–100.
61. Julian LJ. Measures of anxiety: State-Trait Anxiety Inventory (STAI), Beck Anxiety Inventory (BAI), and Hospital Anxiety and Depression Scale-Anxiety (HADS-A). Arthritis Care Res 2011;63 Suppl 11:S467–72.
62. Facco E, Stellini E, Bacci C, et al. Validation of Visual Analogue Scale for Anxiety (VAS-A) in preanesthesia evaluation. Minerva Anestesiol 2013;79:1389–95.
63. Griffith NM, Szaflarski JP, Szaflarski M, et al. Measuring depressive symptoms among treatment-resistant seizure disorder patients: POMS depression scale as an alternative to the BDI-II. Epilepsy Behav 2005;7:266–72.
64. Buysse DJ, Reynolds CF III, Monk TH, Berman SR, Kupfer DJ. The Pittsburgh Sleep Quality Index: a new instrument for psychiatric practice and research. Psychiatry Res 1989;28:193–213.
65. Backhaus J, Junghanns K, Broocks A, Riemann D, Hohagen F. Test-retest reliability and validity of the Pittsburgh Sleep Quality Index in primary insomnia. J Psychosom Res 2002;53:737–40.
66. Buysse DJ, Reynolds CF III, Monk TH, Hoch CC, Yeager AL, Kupfer DJ. Quantification of subjective sleep quality in healthy elderly men and women using the Pittsburgh Sleep Quality Index (PSQI). Sleep 1991;14:331–8.
67. Monk TH, Reynolds CF, Kupfer DJ, et al. The Pittsburgh Sleep Diary. J Sleep Res 1994;3:111–20.
68. Doman J, Detka C, Hoffman T, et al. Automating the sleep laboratory: implementation and validation of digital recording and analysis. Int J Biomed Comput 1995;38:277–90.
69. Newell J, Mairesse O, Verbanck P, Neu D. Is a one-night stay in the lab really enough to conclude? First-night effect and night-to-night variability in polysomnographic recordings among different clinical population samples. Psychiatry Res 2012;200:795–801.
70. Rechtschaffen A, Kales A. A manual of standardized terminology, techniques and scoring system for sleep stages of human subjects. Washington, DC: US Government Printing Office, 1968.
71. Reivich M, Kuhl D, Wolf A, et al. The [18F]fluorodeoxyglucose method for the measurement of local cerebral glucose utilization in man. Circ Res 1979;44:127–37.
72. Nofzinger EA, Price JC, Meltzer CC, et al. Towards a neurobiology of dysfunctional arousal in depression: the relationship between beta EEG power and regional cerebral glucose metabolism during NREM sleep. Psychiatry Res 2000;98:71–91.
73. Ashburner J, Friston KJ. Unified segmentation. Neuroimage 2005;26:839–51.
74. Woods RP, Grafton ST, Holmes CJ, Cherry SR, Mazziotta JC. Automated image registration: I. General methods and intrasubject, intramodality validation. J Comput Assist Tomogr 1998;22:139–52.
75. Hunter GJ, Hamberg LM, Alpert NM, Choi NC, Fischman AJ. Simplified measurement of deoxyglucose utilization rate. J Nucl Med 1996;37:950–5.
76. Gläscher J, Gitelman D. Contrast weights in flexible factorial design with multiple groups of subjects. Accessed June 19, 2016. Available from: http://www.sbirc.ed.ac.uk/cyril/download/Contrast_Weighting_Glascher_Gitelman_2008.pdf.
77. Xia MR, Wang JH, He Y. BrainNet Viewer: a network visualization tool for human brain connectomics. PLoS One 2013;8:e68910.
78. Riemann D, Spiegelhalder K, Feige B, et al. The hyperarousal model of insomnia: a review of the concept and its evidence. Sleep Med Rev 2010;14:19–31.
79. Kattler H, Dijk DJ, Borbély AA. Effect of unilateral somatosensory stimulation prior to sleep on the sleep EEG in humans. J Sleep Res 1994;3:159–64.
80. Smith EE, Jonides J, Marshuetz C, Koeppe RA. Components of verbal working memory: evidence from neuroimaging. Proc Natl Acad Sci USA 1998;95:876–82.
81. Kapur S, Craik FI, Tulving E, Wilson AA, Houle S, Brown GM. Neuroanatomical correlates of encoding in episodic memory: levels of processing effect. Proc Natl Acad Sci USA 1994;91:2008–11.
82. Kircher TT, Senior C, Phillips ML, et al. Towards a functional neuroanatomy of self processing: effects of faces and words. Cogn Brain Res 2000;10:133–44.
83. Fossati P, Hevenor SJ, Lepage M, et al. Distributed self in episodic memory: neural correlates of successful retrieval of self-encoded positive and negative personality traits. Neuroimage 2004;22:1596–604.
84. Buckner RL, Andrews-Hanna JR, Schacter DL. The brain's default network: anatomy, function, and relevance to disease. Ann N Y Acad Sci 2008;1124:1–38.
85. Zhang S, Li CS. Functional connectivity mapping of the human precuneus by resting state fMRI. Neuroimage 2012;59:3548–62.
86. Bench CJ, Friston KJ, Brown RG, Frackowiak RS, Dolan RJ. Regional cerebral blood flow in depression measured by positron emission tomography: the relationship with clinical dimensions. Psychol Med 1993;23:579–90.
87. Wang Y, Zhong S, Jia Y, et al. Interhemispheric resting state functional connectivity abnormalities in unipolar depression and bipolar depression. Bipolar Disord 2015;17:486–95.
88. Mulders PC, van Eijndhoven PF, Schene AH, Beckmann CF, Tendolkar I. Resting-state functional connectivity in major depressive disorder: a review. Neurosci Biobehav Rev 2015;56:330–44.

89. Kyle SD, Beattie L, Spiegelhalder K, Rogers Z, Espie CA. Altered emotion perception in insomnia disorder. Sleep 2014;37:775–83.
90. Holbrook AM, Crowther R, Lotter A, Cheng C, King D. The diagnosis and management of insomnia in clinical practice: a practical evidence-based approach. CMAJ 2000;162:216–20.
91. Morin CM, Culbert JP, Schwartz SM. Nonpharmacological interventions for insomnia: a meta-analysis of treatment efficacy. Am J Psychiatry 1994;151:1172–80.
92. Ong JC, Manber R, Segal Z, Xia Y, Shapiro S, Wyatt JK. A randomized controlled trial of mindfulness meditation for chronic insomnia. Sleep 2014;37:1553–63.
93. Jiang CG, Zhang T, Yue FG, Yi ML, Gao D. Efficacy of repetitive transcranial magnetic stimulation in the treatment of patients with chronic primary insomnia. Cell Biochem Biophys 2013;67:169–73.
94. Buchsbaum MS, Gillin JC, Wu J, et al. Regional cerebral glucose metabolic rate in human sleep assessed by positron emission tomography. Life Sci 1989;45:1349–56.
95. Heiss WD, Pawlik G, Herholz K, Wagner R, Wienhard K. Regional cerebral glucose metabolism in man during wakefulness, sleep, and dreaming. Brain Res 1985;327:362–6.
96. Bastien CH. Insomnia: Neurophysiological and neuropsychological approaches. Neuropsychol Rev 2011;21:22–40.
97. Krueger JM, Huang YH, Rector DM, Buysse DJ. Sleep: a synchrony of cell activity-driven small network states. Eur J Neurosci 2013;38:2199–209.
98. Kay DB, Soehner AM, Hasler BP, et al. Neurobiological basis for insomnia disorder: smaller wake-NREM sleep reductions in regional brain glucose metabolism compared to good sleepers. Sleep 2015;38 (Abstract Suppl):A242–3.

ACKNOWLEDGMENTS

The authors thank Jean Miewald and Mary Fletcher for database management. The authors acknowledge with gratitude the dedicated work and technical skills provided by University of Pittsburgh staff at the Neuroscience Clinical and Translational Research Center, the Positron Emission Tomography Center, the Sleep and Chronobiology Faculty, the General Clinical Research Center, Sleep Imaging Research Program, and the Clinical Neuroscience Research Center. The authors thank the many polysomnographic technologists who conducted the overnight sleep studies for the protocols reported in this paper including Dori Adams, Linda Bankson, Denise Duryea, Rachel Huff, Denny Knorr, Dan Limpert, Nancy Lutheran, Eric Miller, Jim Monahan, Kristen Page, Nicole Patton, Karen Quigley, Michael Quigley, Sarah Rankin, Steve Swanger, John Thase, Sarah Thase, Anne Vaniea, F. Jay Ver, and Monica Winkelman.

SUBMISSION & CORRESPONDENCE INFORMATION

Submitted for publication November, 2015
Submitted in final revised form May, 2016
Accepted for publication May, 2016
Address correspondence to: Daniel J. Buysse, MD, Sleep and Chronobiology Faculty, Western Psychiatric Institute and Clinic, 3811 O'Hara Street, Room E-1127, Pittsburgh, PA 15213; Tel: (412) 246-5300; Fax: (412) 246-6413; Email: buyssedj@upmc.edu

DISCLOSURE STATEMENT

Dr. Buysse had full access to all of the data in the study and takes responsibility for the integrity of the data and the accuracy of the data analysis. Preliminary results using subsets of participants reported in this study have been previously published in review articles[32,33,97] and abstracts[98] but data from 50% of participants included in this study have not been previously analyzed. One of the protocols included in these analyses was supported by Sepracor, Inc. That protocol contributed 6 participants to this study. The remaining protocols used in this study were not industry-supported. Dr. Nofzinger is on the Board of Directors and is Chief Medical Officer for Cerêve, Inc. Dr. Buysse is a paid consultant to Cerêve, Inc., Emmi Solutions, and Merck. Dr. Aizenstein has received research support from Novartis Pharmaceuticals. Dr. Kay was supported by T32HL082610 (PI: Buysse), Dr. Soehner was supported by T32MH018269 (PI: Pilkonis), Dr. Wilckens was supported by T32MH019986 (PI: Reynolds) and K01AG049879, and Dr. Hasler was supported by K01DA032557. The other authors have indicated no conflicts of interest.